33RD International Association of Hydraulic Engineering & Research Congress, IAHR
Vancouver, British Columbia, Canada. August 10 – 14, 20009

MEASUREMENT OF VELOCITIES AND CHARACTERIZATION OF SOME PARAMETERS INSIDE OF FREE AND SUBMERGED HYDRAULIC JUMPS

Luis G. Castillo E [1]

[1]Department of Thermic and Fluids Engineering, Technical University of Cartagena,
E.U. Civil Engineering, Paseo Alfonso XIII, 52, 30203 Cartagena, Spain,
phone: +34 968 327012; fax: +34 968 325435; e-mail: luis.castillo@upct.es

ABSTRACT

Measurement of instantaneous velocities with ADV equipment, are very reliable in laminar and turbulent flows without the air presence, because the water constitutes the fundamental element of sound transmission.
However, in two-phase flows (water-air), for example inside of a hydraulic jump, the register measurements can be wrong when air bubbles pass through the measurement volume, because in this instant the sound echo is not correctly transmitted.
In these circumstances it is necessary to verify the registers and to carry out a digital filtering of the information, in order to eliminate and/or correct the anomalous data but maintaining the continuity of the register.
In this paper are analysed some digital filters and applied to the registers of instantaneous velocities measurements inside of some configurations of free and submerged hydraulic jump. The obtained results are compared and contrasted with the already supported experimental and theoretical results.

Keywords: Acoustic Doppler Velocimeter, turbulent high two-phase flow, digital filtering

TOPIC A-5. Laboratory experiments, instrumentation, and hydraulic modelling

INTRODUCTION

Acoustic Doppler Velocimeters (ADV) have become very useful in fluid dynamics and they are applied to the study of the three-dimensional flow and turbulence in laboratory, as well as in the field (rivers, channels, hydraulic structures, etc.).
ADV typically consists of one emitter surrounded by a number of receivers, each of them measuring one projections of the velocity vector. The emitter generates an acoustic wave of frequency f_e with speed of the sound c and wavelength $\lambda_e = c / f_e$ that propagates through the fluid, is scattered by acoustic targets moving with the fluid velocity u, and finally is detected by the receiver. Due to the target u, the wavelength λ_r and the corresponding frequency $\lambda_r = c / f_r$ of the scattered acoustic wave differ from those of the emitted one; the Doppler frequency is defined as the frequency shift of the acoustic wave, induced by the moving target $f_D = f_r - f_e$.
The relation between the Doppler frequency and the projections of the target velocity u along the emitter and receiver axes, u_e and u_r, is $f_D = f_c / c(u_e + u_r)$.

ADV measure the velocity of acoustic targets moving with the fluid, rather than directly the fluid velocity. Since these acoustics targets follow the fluid motion with negligible inertial lag, their velocity is assumed to be identical to the fluid velocity.
ADVs are able to measure the time-averaged flow field with an accuracy that is better than 4%. High resolution ADV measurements of turbulence are only possible with pulse-to-pulse coherent instruments, however, the signal suffers from parasitical noise contributions and this noise has the following characteristics (Blanckaert and Lemin, 2006):

- Its energy content is uniformly distributed over the investigated frequency domain (white noise).
- It is unbiased: $\overline{\sigma_i} = 0$. Therefore, it does not affect the estimates of the time-averaged velocity $\overline{u}$.
- It is statistically independent of the corresponding true Doppler frequency: $\overline{\sigma_i f_{D,i}} = 0$ if $i \neq j$.
- The noise of the different receivers is statistically independent: $\overline{\sigma_i \sigma_j} = 0$. Then noise-free estimates of the turbulent shear stress are obtained if $\overline{\sigma_i^2} = \overline{\sigma_j^2} = \overline{\sigma}^2$. However, the estimates of the turbulent normal stress, are affected by noise.

The spikes in ADV time series can be caused by many factors, including high turbulent intensities, aerated flows that have undesirable acoustic properties, and phase difference ambiguities that occur when the velocities exceed the upper limits of ADV probe velocity range. Although spikes can be reduced or eliminated in many cases by adjustment of probe operational parameters, there are some situations in which spikes cannot be entirely avoided (Wahl, 2003).
A hydraulic jump is characterized by a sudden rise of the free-surface, with strong energy dissipation and mixing, large-scale turbulence, air entrainment, waves and spray. So, in two-phase-flows (water-air), the register measurements can be wrong when air bubbles pass through the measurement volume and in this instant, the sound echo is not correctly transmitted. In these circumstances, it is necessary to verify the registers and to carry out a digital filtering of the information, in order to eliminate and/or correct the anomalous data but maintaining the continuity of the register.
In this paper are analysed some digital filters and applied to the registers of instantaneous velocities measurements inside of some configurations of free and submerged hydraulic jump. The results obtained are compared and contrasted with the already supported experimental and theoretical results.

METHODS

Despiking involves two steps: (1) detecting the spike and (2) replacing the spike. The two steps are independent but for the iterative methods, spike replacement can affect spike detection in the subsequent iterations.
There are some spikes detection algorithms. In this work we apply the following ones:

- Acceleration Thresholding Method (Nikora and Goring 2000 and modified in this paper).
- Progressive cut of the lower and upper limits in function of 5 and 95% statistical (Castillo 2008).
- Phase-Space Thresholding Method (Goring and Nikora 2002 as modified in Wahl 2003).

Acceleration Thresholding Method (ATM+C)

In order to a point be a spike, the acceleration must exceed a threshold $\lambda_a g$ and the absolute deviation from the mean velocity of the point must exceed $k\sigma$, where λ_a is a relative acceleration threshold, σ is the standard deviation and k is a factor to be determined. This method is a detection and replacement procedure with two phases: one for negative accelerations and the second for positive accelerations. In each phase, numerous passes through the data are made until all data points conform to the acceleration criterion $\lambda_a g$ and the magnitude threshold $k\sigma$. The steps in each phase are:

1. Calculate the acceleration from $a_i = (u_i - u_{i-1})/\Delta t$, where u_i is discrete velocity time series and Δt the sampling interval;
2. Indentify those points where $a_i < -\lambda_a g$ and $u_i < -k\sigma$ and replace them.

Step 2 is repeated until no more spikes are detected, then the second phase is begun:

1. Calculate the acceleration as above; and
2. Identify those points where $a_i > \lambda_a g$ and $u_i > k\sigma$ and replace them.

Step 2 is repeated until no more spikes are detected.

Nikora and Goring 2000 indicate that good choices for the parameters are: $\lambda_a = 1 - 1.5$ and $k = 1.5$.

However, we have observed that for hydraulic jump cases the λ_a value must be calculated in function of the *j* section position (d_j) inside of hydraulic jump and its corresponding Froude number, Fr_j. Then the acceleration a_j in function of Froude number is:

$$a_j = \frac{u_j}{\Delta t} = \frac{Fr_j \sqrt{g y_j}}{\Delta t} = \lambda_{aj} g \qquad (1)$$

Where $\lambda_{aj} = Fr_j \sqrt{y_j} / (\Delta t \sqrt{g}) \geq 0.5$, Δt is time interval between data points, y_j takes the depth value y_{dj} when the flow is downstream and y_{uj} when the flow is upstream (see Figure 1). In this way, the parameter λ_{aj} is established by the flow specific characteristics in each section of measurement.

The threshold k that is usually applied arises from a theoretical result from normal probability distribution theory which says that for *n* independent, identically distributed, standard, normal, random variable ξ_i, the expected absolute maximum is:

$$E(|\xi_i|_{\max}) = \sqrt{2 \ln n} = \lambda_U \qquad (2)$$

Where λ_U is denominated the Universal threshold. For a normal, random variable whose standard deviation is estimated by σ and the mean zero, the expected absolute maximum is

$$\lambda_U \sigma = \sqrt{2 \ln n}\, \sigma \qquad (3)$$

However, this threshold can result very wide when the time distribution is not normal, as in the case of the velocities distribution inside of a hydraulic jump.

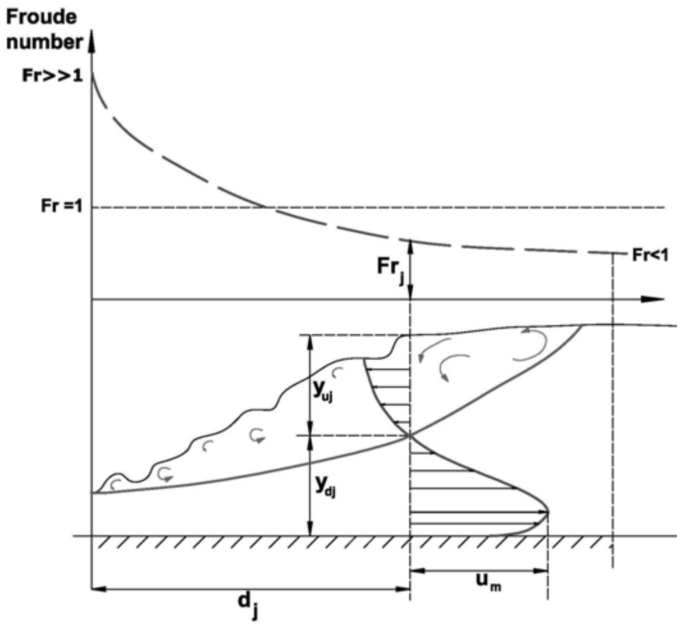

Figure 1 Froude number variation and principal parameters inside of hydraulic jump.

Progressive cut of the lower and upper limits in function of 5% and 95% statistical (PCLU)

The method is based on the above conclusion. So, because the velocity time distribution does not fit a normal distribution, then it is better to estimate a threshold trends to the upper limit really registered in the signal. The data filtering is based on progressive cut of the lower and upper limits, in function of the 5 % and 95 % statistical (Castillo 2008). From the mean, $\bar{u}$ and maximum, $u_{\max}$ values registered in the data series, the first relative amplitude is determined, $A_1 = u_{\max} - \bar{u}$. Next is found the value $u_{mín} = \bar{u} - A_1$ and the general amplitude $A = u_{\max} - u_{mín}$. Finally they are obtained the superior cut value, $X_{máx.c}$ and the lower cut value, $X_{mín.c}$ from the initial series, so that $X_{máx.c} = u_{\max} - (0.05A)$ and $X_{mín.c} = u_{mín} + (0.05A)$.
This process can be repeated if the data series need it. However it is recommended not to do more than two filtering data, so that the initial series be little altered. In the method the spike is replaced automatically by the upper or lower value of the corresponding cut. However, as an alternative, the spike can be replacement by the sample median.

Phase-Space Thersholding Method (PSTM+W)

The method uses the concept of a three-dimensional Poincaré map or phase-space plot in which the variable and its derivatives are plotted against each other. The points are enclosed by an ellipsoid defined by the Universal criterion and the points outside the ellipsoid are designated as spikes. The method iterates until the number of good data becomes constant (Goring and Nikora 2002). Each iteration has the following steps:

1. Calculate surrogates for the first and second derivatives from central differences algorithm:

$$\Delta u_i = (u_{i+1} - u_{i-1})/2 \qquad (4)$$

$$\Delta^2 u_i = (\Delta u_{i+1} - \Delta u_{i-1})/2 \qquad (5)$$

Note that is not divided by time step Δt to ensure that Eqs. (7) and (8) do not become ill conditioned.

2. Calculate the standard deviations of all three variables, σ_u, $\sigma_{\Delta u}$, and $\sigma_{\Delta 2u}$, and thence the expected maxima using the Universal criterion.
3. Calculate the rotation angle of the principal axis of $\Delta^2 u_i$ versus u_i using the following cross correlation $\theta = \tan^{-1}\left(\sum u_i \Delta^2 u_i / \sum u_i^2\right)$. However, we propose a new relation obtained by the Gauss´ fit:
$$\theta = \tan^{-1}\left[(n\sum u_i \Delta^2 u_i - \sum u_i \sum \Delta^2 u_i)/(n\sum u_i^2 - (\sum u_i)^2)\right] \qquad (6)$$
4. For each pair of variables, calculate the ellipse that has maxima and minima from point 3. Thus, for Δu_i versus u_i the major axis is $\lambda_U \sigma_u$ and the minor axis is $\lambda_U \sigma_{\Delta u}$; for $\Delta^2 u_i$ versus Δu_i the major axis is $\lambda_U \sigma_{\Delta u}$ and the minor axis is $\lambda_U \sigma_{\Delta 2u}$; and for $\Delta^2 u_i$ versus u_i the major and minor axes, *a* and *b*, respectively, are the solutions of $(\lambda_U \sigma_U)^2 = a^2 \cos^2\theta + b^2 \sin^2\theta$ and $(\lambda_U \sigma_{\Delta 2u})^2 = a^2 \sin^2\theta + b^2 \cos^2\theta$.
In this paper are proposed the following equations systems:
$$(\lambda_U \sigma_U)^2 = a^2 \cos^2(\theta/2) + b^2 (\lambda_U \sigma_u / \lambda_U \sigma_{\Delta 2u})^2 \sin^2(\theta/2) \qquad (7)$$
$$(\lambda_U \sigma_{\Delta 2u})^2 = a^2 (\lambda_U \sigma_{\Delta 2u} / \lambda_U \sigma_u)^2 \sin^2(\theta/2) + b^2 \cos^2(\theta/2) \qquad (8)$$
5. For each projection in phase space, identify the points that lie outside of the ellipse and replace them.

At each iteration, replacement of the spikes reduces the standard deviation calculated in 2 and thus the size of the ellipsoid.

This despiking algorithm uses the mean and standard deviation, the classic estimators for locations and scale, respectively. However, a single outlier of extraordinary magnitude can corrupt both parameters and affect significantly the performance.

Wahl 2003 proposed the sample median as an estimator of location and, the median of the absolute deviations from the sample median (MAD), as estimator of scale. He added to the WinADV computer program (Wahl 2000) the modified algorithm incorporating among others the following features:

- The median and MAD are used as location and scale estimators.
- Chauvenet´s criterion is used to define the rejection probability and exclusions thresholds.
- Despiking is carried out on each of the available velocity components, and all associated data are removed when a spike is detected in any one of the time series.

APPLICATION AND CONCLUSIONS

Figure 2 shows two horizontal velocity register obtained inside of a hydraulic jump in identical conditions of position and flow. The registers were obtained with a rate of data acquisition of 5 points per second and, the unique difference consisted in that the velocity range of the left register was ± 100 cm/s, so, the theoretical horizontal maximum velocity is ± 300 cm/s and, for the right register, ± 250 cm/s (horizontal maximum velocity of ± 360 cm/s).

The left register is very contaminated and, although the maximum velocity registered is lower than the half of the maximum permitted in flow normal conditions, however, in the extreme conditions of the flow inside of hydraulic jump, numerous spikes are produced by phase difference ambiguities and, these are due to that the real upper limit of velocity is very much low. This register is a pathological case that we would reject. However, we have the opportunity to test the different algorithms.
The right figure is a clean register and it constitutes the same left register without spikes by phase difference ambiguities. The spikes that contain this register would be exclusively due to aeration problems.
Table 1 shows a resume and comparison of the principal obtained results.

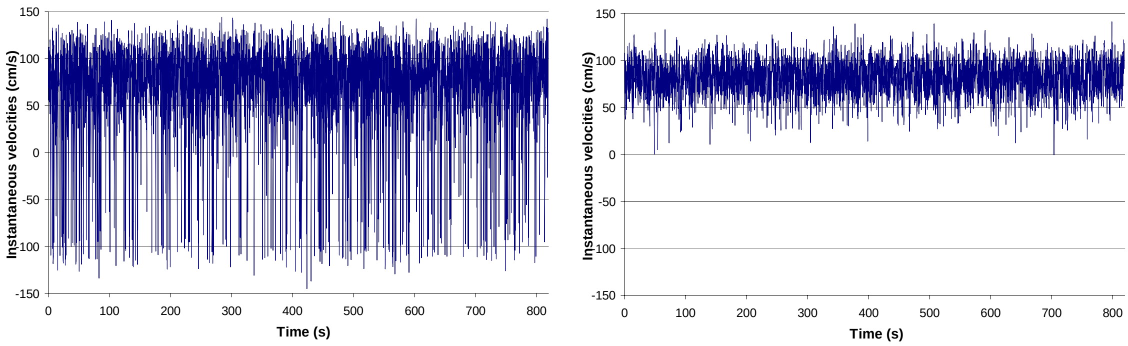

Figure 2 Types of velocity registers. Left: pathological register. Right: clean register.

In the case of the clean register, all the methods give similar results in the sample mean after of filtering and, are a bit higher than the mean value of the original series.
However, the standard deviations are reduced over the five percent after of filtering. This circumstance indicates that the turbulence normal stress is not correct and, we would be able to discriminate the real stress from the white noise. Hurther and Lemmin (2001) have proposed a direct correction method by which most of the noise in turbulence measurements with four-receiver ADV instruments can be eliminated, in function of the redundant information on one velocity component.
It is interesting to note that for the case of velocities registered inside of hydraulic jump, the combination ATM+C and PCLU methods constitute the more robust procedure of filtering. We can observe that the mean value and the standard deviation are the most similar to the original series values and, is the only procedure that let us obtain the mean value from the pathological register, with an error lower that 1%.

Table 1 Comparison of results obtained by the application of different filtering methods.

	Pathological register	Clean register
Length of time series:	4504	4504
Time interval between data point (s):	0.20	0.20
Sample mean (cm/s):	69.56	81.56
Standard deviation (cm/s):	52.73	18.63
ATM+C method	2 iterations	1 iteration
Spikes identified:	816	84
Sample mean after of filtering:	80.89	81.63
Standard deviation after of filtering:	26.17	18.32
PSTM+W method	2 iterations	1 iteration

Spikes identified: Sample mean after of filtering: Standard deviation after of filtering:	1457 72.25 24.91	679 78.12 17.66
ATM+C and PSTM+W methods	ATMC+C:2 iterations PSTM+W:1 iterations	ATMC+C:2 iterations PSTM+W:1 iterations
Spikes identified: Sample mean after of filtering: Standard deviation after of filtering:	1637 77.20 21.25	795 78.01 17.64
ATM+C and PCLU methods	ATMC+C:2 iterations PSTM+W:1 iterations	ATMC+C:2 iterations PSTM+W:0 iterations
Spikes identified: Sample mean after of filtering: Standard deviation after of filtering:	1082 81.45 23.12	289 81.63 18.32

From systematic application of the ATM+C and PCLU methods to the time registers of velocities in different sections inside of free and submerged hydraulic jumps (Figure 3a) and, from analysis of the mean velocity experimental distribution, it was obtained a similar velocity distribution, in the range [$0.2\leq x/L_j \leq 0.7$], (Figure 3b).

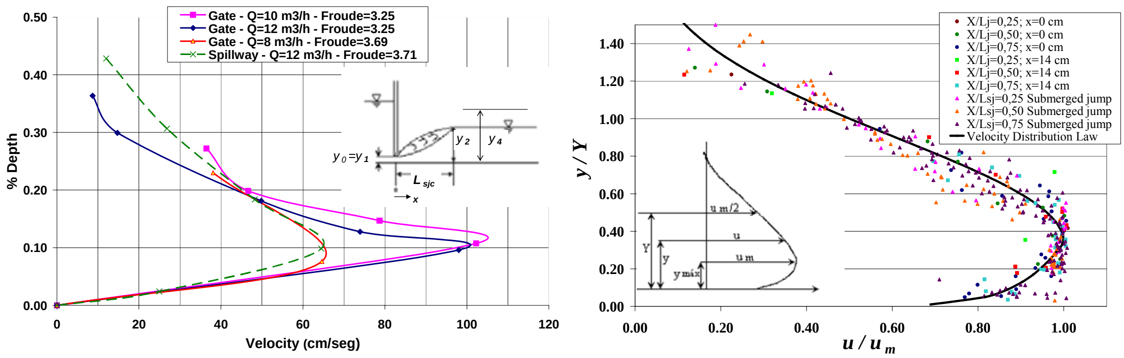

Figure 3 (a) Velocity distributions in the middle of hydraulic jump.
(b) Velocity distribution law inside of free and submerged hydraulic jumps.
Validity range: $2.5\leq F_{r1}\leq 5$; $0.25\leq x/L_{sjc}\leq 0.75$ y $4\leq y_4/y_0\leq 10$.

The scalar length, Y, is the depth where the velocity is equal to the half of the registered maximum velocity, $\bar{u} = u_m/2$, and, $y_{máx}$, is the depth where $\bar{u} = u_m$.
The best fit of the velocity distribution law inside of free and submerged hydraulic jumps are:

$$\frac{\bar{u}}{u_m} = \{\frac{1}{k}(\frac{y}{Y})\}^{1/n};\quad 0\leq \frac{y}{Y}\leq k \qquad (10)$$

$$\frac{\bar{u}}{u_m} = \exp[-\frac{1}{2}\{\frac{1.177}{1-k}(\frac{y}{Y}-k)\}^2];\quad k\leq \frac{y}{Y}\leq 1.5 \qquad (11)$$

Where, $k = y_{máx}/Y$.

Table 2 shows the coefficient, k, exponent, n, and the corresponding validity ranges of the velocity distribution law in free and submerged hydraulic jumps. It is interesting to note that the difference in the characteristics of developing and developed flow, are completely diffused inside of hydraulic jump. This last phenomenon is produced because the turbulence diffuses all flow characteristics such as momentum, energy or even turbulence itself (Rouse et al., 1959). The present results constitute complementary laws of the proposed by Ohtsu et al. (1990).

Table 2 Coefficient, *k*, and exponent, *n*. Velocity distribution law in hydraulic jumps.

Velocity distribution law	Range of application	*k*	*n*
Free and submerged hydraulic jump Undeveloped flow Castillo (2008)	$2.5 \le F_1 \le 5$ $0.25 \le x/L_{jc} \le 0.75$ $4 \le y_4/y_0 \le 10$	0.342	9.5
Free hydraulic jump. Undeveloped flow Ohtsu et al. (1990)	$5 \le F_1 \le 7.3$ $0.2 \le x/L_{jc} \le 0.7$	0.333	12
Free hydraulic jump. Developed flow Ohtsu et al. (1990)	$5.3 \le F_1 \le 7.3$ $0.2 \le x/L_{jc} \le 0.7$	0.351	7

REFERENCES

Blanckaert, K. and Lemmin, U. (2006), Means of noise reduction in acoustic turbulence measurements. Journal of Hydraulic Research Vol. 44, No. 1, pp. 3-17.

Castillo, L. (2008), Validation of instantaneous velocities measurements with ADV equipment in turbulent high two-phase flows. The Eight Int. Conference on Hydro-Science and Engineering (ICHE 2008). Nagoya, Japan, Sep 8-12.

Chanson, H. (2005), Air bubble entrainment in hydraulic jumps. Similitude and scale effects. The University of Queensland, Department of Civil Engineering, Report CH57/05.

Goring, G. and Nikora, V.(2002), Despiking acoustic Doppler velocimeter data. Proc. ASCE, Journal of Hydraulic Engineering, Vol. 128, Nº 1, January 1. pp. 117-126.

Hurther, D. and Lemmin, U. (2001), A correction method for turbulence measurements with a 3-D acoustic Doppler velocity profiler. J. Atmos. Ocean. Technol. 18, 446-458.

Márquez, C. (2006), Caracterización paramétrica de resaltos hidráulicos libres y sumergidos a partir de medidas de velocidades instantáneas con equipo Doppler. Proyecto Fin de Carrera. EU de Ingeniería Civil. Universidad Politécnica de Cartagena, UPCT, Spain.

Ohtsu, F., Yasuda, Y. and Awazu, S. (1990), Free and submerged hydraulic jumps in rectangular channels. Report of the Research Institute of Science and Technology, Nihon University, No 35.

Rouse, H., Siao, T.T. and Nagaratnam, S. (1959). Turbulence characteristics of the hydraulic jump. Trans. ASCE 124: pp. 926-966.

Vischer, D.L. and Hager, W.H. (1995), Energy Dissipators. No 9 Hydraulic Structures Design Manual, *International Association for Hydraulic Research*, IAHR. Taylor & Francis Group.

Wahl, T. L. (2000), Analyzing ADV data using WinADV. Proc., 2000 Joint Conference on Water Resources Engineering and Water Resources Planning and Management, ASCE, July 30-Agust 2, Minnneapolis, www.usbr.gov/wrrl/twahl/winadv.

Wahl, T. L. (2003), Discussion of “Despiking acoustic Doppler velocimeter data” by Derek G. Goring and Vladimir I. Nikora. January 2002, Vol. 128, No 1, pp. 117-126. Proc. ASCE, Journal of Hydraulic Engineering, June 1. pp. 484-488.